Importance of tetrahedral coordination for high-valent transition-metal oxides: $YCrO_4$ as a model system

A. A. Tsirlin,[1,2] M. G. Rabie,[1,3,4] A. Efimenko,[1,4] Z. Hu,[2] R. Saez-Puche,[3] and L. H. Tjeng[1]

[1]*Max Planck Institute for Chemical Physics of Solids, Nöthnitzer Straße 40, 01187 Dresden, Germany*

[2]*National Institute of Chemical Physics and Biophysics, 12618 Tallinn, Estonia*

[3]*Departamento Quimica Inorganica, Facultad de Ciencas Quimicas, Universidad Complutense de Madrid, 28040 Madrid, Spain*

[4]*II. Physikalisches Institut, Universität zu Köln, Zülpicher Straße 77, 50937 Köln, Germany*

(Received 25 October 2013; revised manuscript received 19 July 2014; published 8 August 2014)

We have investigated the electronic structure of the high oxidation state material $YCrO_4$ within the framework of the Zaanen-Sawatzky-Allen phase diagram. While Cr^{4+}-based compounds such as $SrCrO_3$/$CaCrO_3$ and CrO_2 can be classified as small-gap or metallic negative-charge-transfer systems, we find using photoelectron spectroscopy that $YCrO_4$ is a robust insulator despite the fact that its Cr ions have an even higher formal valence state of 5+. We reveal using band-structure calculations that the tetrahedral coordination of the Cr^{5+} ions in $YCrO_4$ plays a decisive role, namely to diminish the bonding of the Cr 3*d* states with the top of the O 2*p* valence band. This finding not only explains why the charge-transfer energy remains effectively positive and the material stable, but also opens up a new route to create doped carriers with symmetries different from those of other transition-metal ions.

DOI: 10.1103/PhysRevB.90.085106 PACS number(s): 71.27.+a, 71.30.+h, 72.80.Ga, 79.60.−i

The nature of the lowest-energy charge excitations in strongly correlated transition-metal compounds is largely determined by the magnitude of the Coulomb energy U at the transition-metal d shell and that of the charge-transfer energy Δ needed to transfer an electron from the d shell to the ligand p states. As pointed out by Zaanen, Sawatzky, and Allen (ZSA) [1], systems with sufficiently large U and Δ values are magnetic insulators, and can be classified as either Mott-Hubbard insulators (the lowest-energy intersite charge excitation is between the d ions) or charge-transfer insulators (the excitation is between the d and p ions). Compounds with small or close-to-negative Δ values can be metallic with p-type charge carriers, and CrO_2 [2–4] as well as Cr^{4+} compounds in general [5–9] are representative for such a case.

One may expect that increasing the Cr valence further to 5+ could result in a truly negative-Δ system. This idea is based on a simple argument that Δ_{n+1} is given by $\Delta_n - U$, where n enumerates the valence [1]. Surprisingly, $YCr^{5+}O_4$ and related $RCrO_4$ compounds with rare-earth R^{3+} ions seem to be insulators according to their deep green color [10–15]. This insulating behavior becomes even more puzzling when a band gap analysis, as developed by Torrance [16], is carried out to include the actual crystal structure effects on the Madelung potentials (Table I). We find that the charge-transfer energy should be negative enough to stabilize a metallic state in $YCrO_4$. Our analysis should also be applicable to $Sr_3Cr_2O_8$ and $Ba_3Cr_2O_8$, which are insulators as well [17–21].

To resolve this issue, we have performed a photoelectron spectroscopy study on the valence band of $YCrO_4$ and combined it with *ab initio* and parametrized band-structure calculations. Experimental results evidence that $YCrO_4$ is a robust insulator. From the calculations, we discover that the tetrahedral coordination of the Cr^{5+} ions plays a crucial role in diminishing the bonding of the Cr 3*d* states with the top of the O 2*p* valence band as to make the charge-transfer energy positive, to allow for the formation of a large band gap, and to keep the compound stable. Additionally, this lack of bonding with the top of the valence band opens new ways to create charge carriers by doping. Such carriers should have a high oxygen character with a symmetry decoupled from that of the transition-metal ions, and possibly generate unexpected phenomena.

We focus on the tetragonal zircon-type polymorph of $YCrO_4$, for which well-characterized bulk samples are available. This compound develops a ferromagnetic order below $T_C = 9$ K [13] and its crystal structure (Fig. 1) comprises isolated $Cr^{5+}O_4$ tetrahedra and $Y^{3+}O_8$ bisdisphenoids zigzag chains. We calculated the Madelung potentials at the O and Cr sites using the TETR utility [22]. The potentials are listed in Table I together with those of $NaCrO_3$, $SrCrO_3$, and $LaCrO_3$ as reference systems for Cr^{5+}, Cr^{4+}, and Cr^{3+} materials, respectively. The calculations for the latter 113 perovskite-type compounds were all done in the idealized cubic crystal structure of $LaCrO_3$ with the same lattice parameter of $a = 3.88$ Å.

Torrance [16] introduced an effective charge-transfer parameter Δ_0 that combines different energy terms related to the electron transfer from the d shell of Cr to the p shell of O:

$$\Delta_0 = e\left(V_M^{\mathrm{O}} - V_M^{\mathrm{Cr}}\right) + A^{\mathrm{O}^-} - I_v^{\mathrm{Cr}} - e^2/d_{\mathrm{Cr-O}}, \qquad (1)$$

where V_M are Madelung potentials, $A^{\mathrm{O}^-} = -7.7$ eV is the electron affinity for the O^- ion (equal to the ionization potential of O^{2-}), I_v is the ionization potential of Cr^{v+}, and $d_{\mathrm{Cr-O}}$ is the Cr–O distance that determines the energy of an excitonic excitation in the ionic model. Torrance [16] found empirically that for a wide range of oxides the optical gap follows roughly the relation $E_{\mathrm{gap}} \approx \Delta_0 - 10$ eV. The calculated Δ_0 values would then suggest that, according to this empirical rule, $LaCrO_3$ should be an insulator, while $SrCrO_3$, $NaCrO_3$, and $YCrO_4$ should be metallic. This approach gives consistent results for $LaCrO_3$ (insulator), $SrCrO_3$ (metal [5,9]), and probably also for $NaCrO_3$ (not available so far), but apparently not for $YCrO_4$ as the latter material seems to be an insulator [13].

To determine quantitatively the insulating state of $YCrO_4$, we have carried out an x-ray photoelectron spectroscopy

TABLE I. Madelung potentials V_M of Cr and O, ionization potentials I_v^{Cr} for Cr^{v+}, relevant Cr–O distances $d_{\mathrm{Cr-O}}$, and the resulting effective charge-transfer parameters Δ_0 according to Torrance [16].

	V_M^{Cr} (V)	V_M^{O}(V)	I_v^{Cr} (eV)	$d_{\mathrm{Cr-O}}$ (Å)	Δ_0 (eV)
$LaCrO_3$	−38.4	22.1	31.0	1.94	14.5
$SrCrO_3$	−46.0	24.0	49.1	1.94	5.6
$NaCrO_3$	−53.5	25.8	69.3	1.94	−5.3
$YCrO_4$	−54.9	26.8	69.3	1.66	−4.2

(XPS) experiment. The spectrum was recorded at room temperature in a spectrometer equipped with a Scienta SES-3000 electron energy analyzer and a Vacuum Generators twin crystal monochromatized Al-$K\alpha$ ($h\nu = 1486.6$ eV) source. The overall energy resolution was set to 0.4 eV, as determined using the Fermi cutoff of a metallic silver reference, which was also taken as the zero of the binding energy scale. The base pressure in the spectrometer was 2×10^{-10} mbar and the sample was cleaved *in situ* to obtain a clean surface. A polycrystalline sample of $YCrO_4$ was prepared by solid-state synthesis as described elsewhere [23]. The valence-band (VB) spectrum is displayed in the top panel of Fig. 2. No charging effects were present, which is important to ensure a reliable energy definition.

The top of the valence band is about 0.5 eV away from the Fermi level, thus establishing not only that $YCrO_4$ is a robust insulator, but also that its band gap is at least 0.5 eV. Our VB XPS spectrum is similar but not identical to that of a $LaCrO_4$ thin film [15]. In the latter, for example, the spectrum is shifted 0.5 eV toward lower binding energies, and the top of the valence band is at the Fermi level. We also note that our spectrum reveals clearly the insulating state, while in an earlier XPS study [24] the poorer energy resolution of 1.2 eV does not allow one to decide unambiguously on the presence or absence of spectral weight at the Fermi level.

In order to analyze individual spectral features, we first performed band-structure calculations using the full-potential FPLO code with the basis set of local atomic-like orbitals [25].

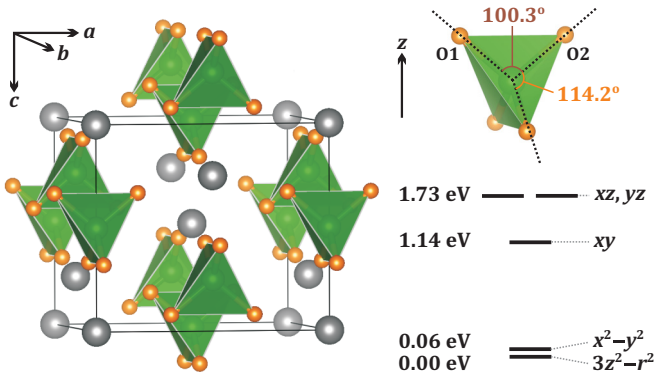

FIG. 1. (Color online) Left panel: Crystal structure of $YCrO_4$ with isolated $Cr^{5+}O_4$ tetrahedra. Right panel: Weak distortion of the tetrahedra and the crystal-field levels with two states of e symmetry ($x^2 - y^2, 3z^2 - r^2$) lying below three states of t_2 symmetry (xy, xz, yz). The energies are given according to LDA with respect to the lowest-lying $3z^2 - r^2$ state.

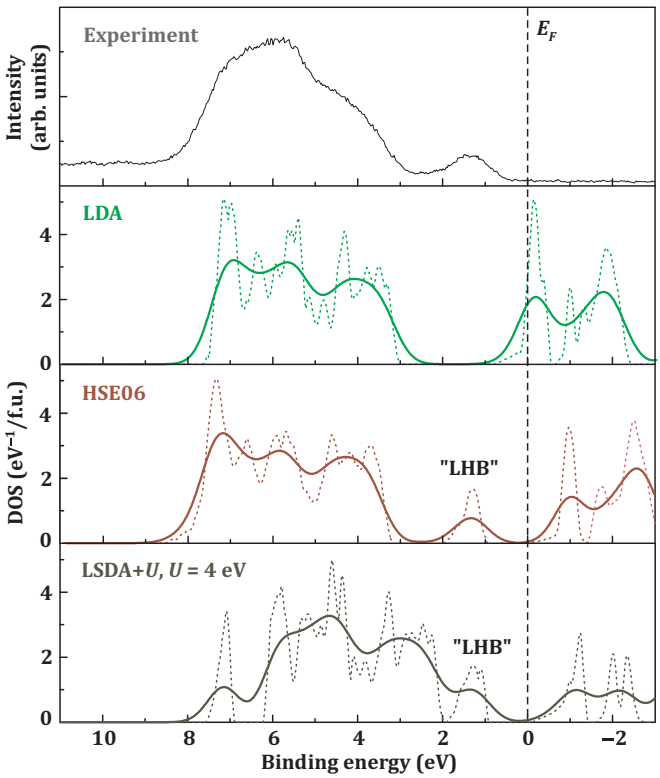

FIG. 2. (Color online) Top panel: Valence-band XPS spectrum of $YCrO_4$. Lower panels: Density of states (DOS) calculated using LDA, HSE06 hybrid functional, and LSDA + U ($U = 4$ eV). Raw DOS curves (dotted lines) are broadened with the experimental resolution (solid lines).

The resulting energy spectrum calculated within the local density approximation (LDA) [26] is depicted in the second-from-top panel of Fig. 2 and shows the anticipated splitting of Cr $3d$ states into the crystal-field levels of the t_2 and e symmetry (compare to the right panel of Fig. 1). Additional splittings related to a weak distortion of the CrO_4 tetrahedra are smaller than the bandwidth.

We can directly conclude that on the LDA level the insulating nature of $YCrO_4$ is not reproduced. The energy splitting between the lowest-energy peak and the broad band at 3–8 eV binding energy is, correspondingly, substantially larger in the calculation. Suspecting that electron correlation effects may play an important role, we took advantage of the Heyd-Scuseria-Ernzerhof (HSE) hybrid-functional approach [27], where a 25% admixture of the exact (Hartree-Fock) exchange to conventional DFT functionals is incorporated. This calculation has been performed in the VASP code [28]. The outcome is extremely encouraging (Fig. 2, bottom): the theoretical spectral line shape and energy positions of all features match very well with that of the experiment. The insulating state is also convincingly reproduced with a calculated band gap of 1.0 eV.

A similar band gap can be obtained in the LSDA + U approach with a properly adjusted U parameter that accounts for Coulomb correlation in the transition-metal d shell on a mean-field level. However, the separation between the narrow band at 1–2 eV and the broad band above 3 eV binding energy

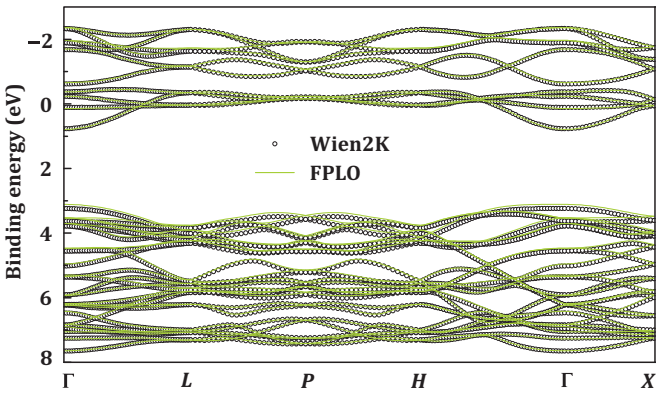

FIG. 3. (Color online) Comparison of LDA band structures calculated in FPLO (lines) and WIEN2K (circles) showing that the choice of the basis set has no influence on the accuracy at the LDA level.

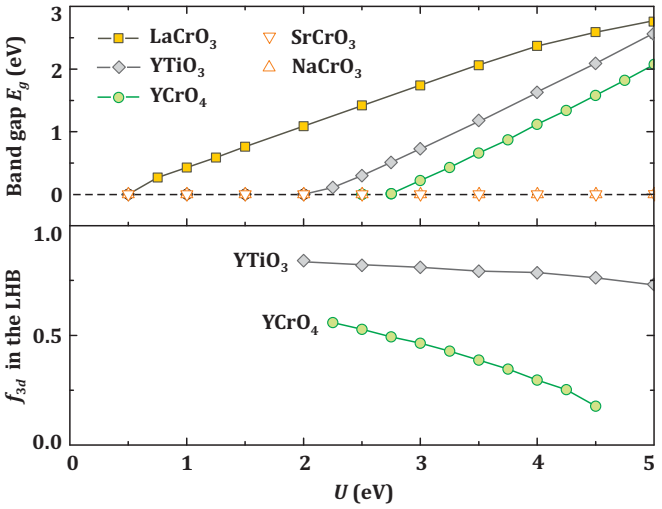

FIG. 4. (Color online) Top panel: LSDA + U band gap E_g as a function of the on-site Coulomb repulsion U in $YCrO_4$ and several reference compounds ranging from the archetype Mott-Hubbard insulator $YTiO_3$ to negative-Δ metals $SrCrO_3$ and $NaCrO_3$. Bottom panel: Fraction of transition-metal $3d$ states (f_{3d}) in the highest occupied state denoted LHB (see Fig. 2). The fractions are calculated by integrating the atomic-resolved DOS. Above $U = 4.5$ eV, the LHB of $YCrO_4$ merges into the oxygen bands, and f_{3d} cannot be determined unambiguously.

is not well reproduced (Fig. 2), because LSDA + U does not correct for the wrong position of oxygen $2p$ levels, which is a well-known problem for a multitude of oxides [29]. This problem is remedied by the hybrid functionals. We note in passing that a similar spectrum of $YCrO_4$ has been reported by Li *et al.* [30], who also used the LSDA + U method but with a much higher U value of 7 eV compared to 4 eV in our calculation. As Li *et al.* [30] used a different band-structure code (WIEN2K) [31], we also performed an LDA calculation in this code and verified that both codes (FPLO and WIEN2K) yield nearly indistinguishable results on the LDA level (Fig. 3). Therefore, we attribute the difference in the value of U to the different basis sets, which then implies that same U has different effect on the orbital occupations depending on the band-structure code and, in particular, on the basis set.

Remarkably, the DOS for $Sr_3Cr_2O_8$ calculated by Radtke *et al.* [17] is, in general, rather similar to that of $YCrO_4$, although the two compounds have quite different crystal structures. We infer a common origin for this, namely, the presence of Cr^{5+} in the tetrahedral oxygen coordination. It has also been pointed out recently that oxide thin films containing Cr ions in the octahedral coordination have very different properties than those having Cr in the tetrahedral coordination [15]. In the following, we will focus on the energy characteristics of the Cr states with the goal to understand how the Cr^{5+} systems can be insulators, and to elucidate why the tetrahedral coordination is a necessity for the stabilization of crystal structures containing high Cr valences.

To place $YCrO_4$ in the ZSA phase diagram [1], we have carried out band-structure calculations, in which we include specifically a parameter U to account for correlation effects in a mean-field manner. Using this so-called LSDA + U approach [32,33], we then investigate how the band gap is affected by a varying magnitude of U. The on-site Hund's exchange parameter is set at its standard value of $J = 1$ eV [6,8,34]. The results are summarized in Fig. 4, and representative energy spectra are shown in Fig. 5. The calculations were performed for $YCrO_4$ together with $LaCrO_3$, $SrCrO_3$, and $NaCrO_3$ as reference systems for different oxidation states of Cr, and for $YTiO_3$ as a reference for a typical Mott-Hubbard insulator. All the calculations assumed ferromagnetic phases, and a simple cubic structure of Cr-based perovskite compounds was chosen in order to simplify the comparison.

Starting with $YTiO_3$ (Fig. 5, right), we can clearly see that a band gap is opened for U larger than 2.0 eV, and this band gap increases linearly with U (Fig. 4). As expected for a typical Mott-Hubbard insulator, a threshold value for U has to be exceeded in order to overcome the one-electron bandwidth W of about 1.9 eV before the insulating state sets in. $LaCrO_3$ has also a band gap that increases linearly with U, and can, therefore, be classified as a Mott-Hubbard insulator as well (Fig. 4). Yet, the threshold value for U is very small (about 0.5 eV) despite a sizable t_{2g} bandwidth of about 2.5 eV, and this can be ascribed to the fact that the gap in this $3d^3$ system is between the Cr t_{2g} and e_g bands, so that the gap is facilitated by the octahedral crystal-field splitting. For $SrCrO_3$, we notice that it does not become insulating for a wide range of U values. A similar finding has been obtained for CrO_2 by Korotin *et al.* [2], who argued that the lack of the band gap in LSDA + U is caused by oxygen $2p$ bands crossing the Fermi level. In CrO_2, the presence of oxygen holes associated with the high oxidation state of Cr in this Cr^{4+} system stabilizes the metallic state. This explanation can also be applied to the metallic regime of $NaCrO_3$ persisting even at very large values of U, since the Cr valence here is extremely high, namely 5+.

Interestingly, the Cr^{5+} system $YCrO_4$ shows a behavior that is in between $YTiO_3$/$LaCrO_3$ on one hand, and $SrCrO_3$/$NaCrO_3$ on the other hand. $YCrO_4$ does become an insulator for large values of U, but only so with a fairly large threshold value of $U = 2.75$ eV (see Fig. 5, left, and Fig. 4). This value is much larger than the one-electron band width of the Cr e bands, which is about 1.3 eV, as can be seen from the LDA panel of Fig. 2. This behavior clearly does not fit

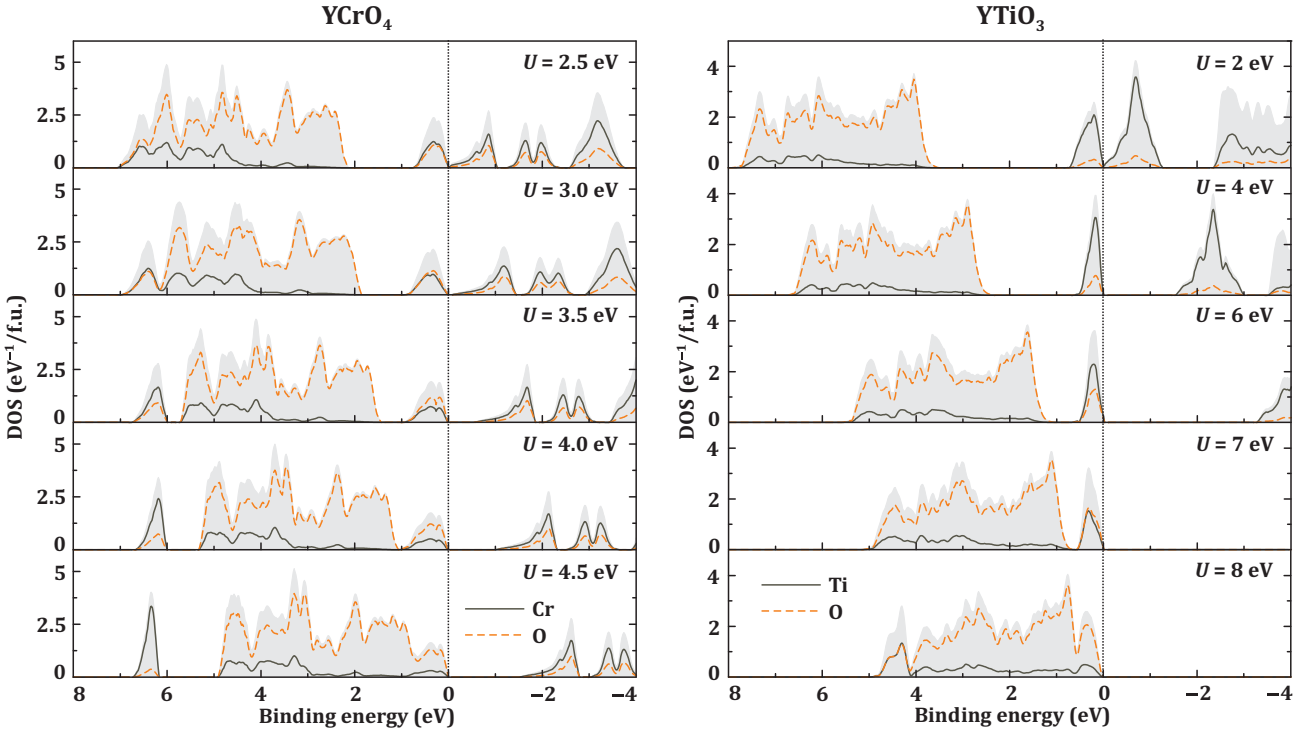

FIG. 5. (Color online) LSDA + U density of states (DOS) calculated for $YCrO_4$ (left panel) and $YTiO_3$ (right panel) for different values of U; only the spin-up channel is shown. Solid and dashed lines are the contributions of the transition-metal (Cr^{5+}, Ti^{3+}) and ligand (O^{2-}) states, respectively. The shading shows the total DOS. The Fermi level is at zero energy and marked by the dotted line that indicates the evolution of $YTiO_3$ from a metal (small U) toward a Mott insulator with a well-defined lower Hubbard band (moderate U), and eventually toward a charge-transfer insulator with the highest occupied states formed by oxygen (large U). In $YCrO_4$, this conventional scenario is altered, because the "lower Hubbard band" of this compound features a large contribution of oxygen even at a low U of 2.5–3.0 eV, where the band gap is just opened.

to that of a classical Mott-Hubbard insulator, despite the fact that the peak at 1.4 eV binding energy seemingly has all the characteristics of being the lower Hubbard band ("LHB"; see Fig. 2).

We now look at the orbital character of this "LHB" as a function of U (Fig. 5), and make a comparison with the $YTiO_3$ case as a reference. The bottom panel of Fig. 4 reveals that for the relevant $U = 4$–5 eV [35] the LHB of $YTiO_3$ has predominantly 3d character and less than one quarter of the O 2p states, thus justifying again the description of $YTiO_3$ as a Mott-Hubbard insulator. For $YCrO_4$, however, we observe a quite different behavior. For low values of U, where the band gap is just opened, the first ionization states are built up of both Cr 3d and O 2p orbitals in about equal amounts. Upon increasing U, the Cr 3d character is reduced and for high values of U, the O 2p nature prevails, even though this spectral feature remains separated from the bulk of the O 2p states. We can, therefore, state that $YCrO_4$ is not a Mott-Hubbard insulator. With a band gap of about 1 eV and a corresponding $U \approx 4$ eV (compare the top panel of Fig. 4 with the experimental band gap of about 1 eV), we would rather classify $YCrO_4$ as a charge-transfer insulator. Consequently, this is also the reason why the opening of the band gap requires a high threshold value of U. The O 2p states are able to push firmly against the "occupied" Cr e band because of the strong hybridization [36]. Therefore, the energy lowering of this "occupied" Cr e band due to U is counteracted, thereby delaying the band gap formation.

Having established the basic characteristics of the electronic structure of $YCrO_4$ in terms of the ZSA diagram, we can now explain why this system is a robust insulator, while the isovalent $NaCrO_3$ and even the lower-valent $SrCrO_3$ and CrO_2 can be classified as negative-charge-transfer p-type metals. Figure 6 shows the partial density of states of $LaCrO_3$, $SrCrO_3$, $NaCrO_3$, and $YCrO_4$, calculated in the nonmagnetic phase using standard LDA. The 113 compounds all have in common that the Cr 3d e_g states hybridize with the bottom half of the O 2p band and that the Cr 3d t_{2g} states tend to hybridize with the top half of the O 2p band, especially in $NaCrO_3$. Partially filled states at the Fermi level have the t_{2g} symmetry. Then the relevant action for the band gap formation is determined by the positions of those t_{2g} orbitals with respect to the O 2p bands with the corresponding t_{2g} symmetry. The relevant energy scale is, therefore, the energy difference between Cr t_{2g} and the *top* of the O 2p band.

Looking now at the $YCrO_4$ case, we can clearly observe that both the Cr 3d t_2 and e bands mix with the *bottom* of the oxygen band. The relevant charge-transfer energy here is then determined by the Cr e states and the *bottom* of the O 2p band. For the 113 compounds, the *effective* charge-transfer energy is reduced by about half of the oxygen bandwidth with respect to the ZSA Δ, which is defined relative to the center of the oxygen band. By contrast, the *effective* charge-transfer energy for $YCrO_4$ is increased by about half of the O 2p bandwidth. The difference between the 113 compounds and $YCrO_4$ is

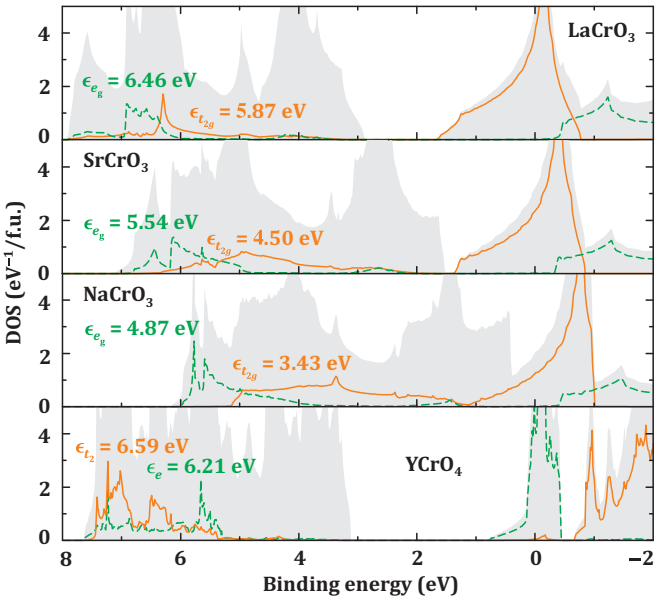

FIG. 6. (Color online) Total (shaded) and Cr orbital-resolved DOS for $YCrO_4$ and reference compounds $LaCrO_3$, $SrCrO_3$, and $NaCrO_3$. The Fermi level is at zero energy. The numbers ϵ_i are relevant centers of gravity for the Cr states hybridized with oxygen.

obviously caused by the difference in the local coordination of the Cr ions. In the 113 compounds, the Cr ions are octahedrally coordinated by oxygens, while in $YCrO_4$ the coordination of Cr is tetrahedral.

The implications may be generalized for transition-metal oxides with only partially filled 3*d* shells: high oxidation state compounds—those with the octahedral coordination of the transition metal—have the potential to feature negative charge-transfer energies and, thus, become metallic, while those with the tetrahedral coordination can still have positive charge-transfer energies and maintain an insulating behavior. Equivalently, one can also state that very high oxidation state materials may have the tendency to build crystal structures with tetrahedral coordination, since the associated increase in the charge-transfer energy ensures the formation of stable insulating states rather than unstable metallic phases with high amount of oxygen holes.

A further intriguing question is the character of charge carriers induced in such compounds by doping. When transition-metal ions have a large effective U, the first ionization state should be positioned at the top of the oxygen band, which is nonbonding. This then leads to the scenario that Korotin *et al.* [2] speculated about in their search for *self-doped* charge carriers in CrO_2. One can then ask how such a particle will interact with the transition-metal ions. Will it form a new quasiparticle with a spin-quantum number, which is very different from that of transition-metal ions, such that a spin-blockade situation occurs [37,38] rendering a high effective mass of this particle? We believe that compounds with the tetrahedral coordination of transition-metal ions deserve further exploration.

We would like to acknowledge fruitful discussions with G. A. Sawatzky, D. I. Khomskii, N. Hollmann, and M. W. Haverkort. A.T. was partly supported by the Mobilitas program of the ESF (Grant No. MTT77). The research in Germany is partially supported by the Deutsche Forschungsgemeinschaft through FOR1346 and the work in Spain by the Marie Curie actions—FP7—through SOPRANO ITN (Grant Agreement No. 214040).

[1] J. Zaanen, G. A. Sawatzky, and J. W. Allen, Phys. Rev. Lett. **55**, 418 (1985).
[2] M. A. Korotin, V. I. Anisimov, D. I. Khomskii, and G. A. Sawatzky, Phys. Rev. Lett. **80**, 4305 (1998).
[3] C. B. Stagarescu, X. Su, D. E. Eastman, K. N. Altmann, F. J. Himpsel, and A. Gupta, Phys. Rev. B **61**, R9233 (2000).
[4] D. J. Huang, L. H. Tjeng, J. Chen, C. F. Chang, W. P. Wu, S. C. Chung, A. Tanaka, G. Y. Guo, H.-J. Lin, S. G. Shyu, C. C. Wu, and C. T. Chen, Phys. Rev. B **67**, 214419 (2003).
[5] L. Ortega-San-Martin, A. Williams, J. Rodgers, J. P. Attfield, G. Heymann, and H. Huppertz, Phys. Rev. Lett. **99**, 255701 (2007).
[6] K.-W. Lee and W. E. Pickett, Phys. Rev. B **80**, 125133 (2009).
[7] A. C. Komarek, S. V. Streltsov, M. Isobe, T. Möller, M. Hoelzel, A. Senyshyn, D. Trots, M. T. Fernández-Dıaz, T. Hansen, H. Gotou, T. Yagi, Y. Ueda, V. I. Anisimov, M. Grüninger, D. I. Khomskii, and M. Braden, Phys. Rev. Lett. **101**, 167204 (2008).
[8] S. V. Streltsov, M. A. Korotin, V. I. Anisimov, and D. I. Khomskii, Phys. Rev. B **78**, 054425 (2008).
[9] A. C. Komarek, T. Möller, M. Isobe, Y. Drees, H. Ulbrich, M. Azuma, M. T. Fernández-Díaz, A. Senyshyn, M. Hoelzel, G. André, Y. Ueda, M. Grüninger, and M. Braden, Phys. Rev. B **84**, 125114 (2011).
[10] E. Jiménez, J. Isasi, and R. Sáez-Puche, J. Alloys Compd. **312**, 53 (2000).
[11] Y. Aoki, H. Konno, and H. Tachikawa, J. Mater. Chem. **11**, 1214 (2001).
[12] R. Sáez-Puche, E. Jiménez, J. Isasi, M. T. Fernández-Díaz, and J. L. García-Muñoz, J. Solid State Chem. **171**, 161 (2003).
[13] Y. W. Long, L. X. Yang, Y. Yu, F. Y. Li, R. C. Yu, and C. Q. Jin, Phys. Rev. B **75**, 104402 (2007).
[14] D. Errandonea, R. Kumar, J. López-Solano, P. Rodríguez-Hernández, A. Muñoz, M. G. Rabie, and R. S. Puche, Phys. Rev. B **83**, 134109 (2011).
[15] L. Qiao, H. Y. Xiao, S. M. Heald, M. E. Bowden, T. Varga, G. J. Exarhos, M. D. Biegalski, I. N. Ivanov, W. J. Weber, T. C. Droubaya, and S. A. Chambers, J. Mater. Chem. C **1**, 4527 (2013).
[16] J. B. Torrance, P. Lacorre, C. Asavaroengchai, and R. M. Metzger, Physica C **182**, 351 (1991).
[17] G. Radtke, A. Saúl, H. A. Dabkowska, G. M. Luke, and G. A. Botton, Phys. Rev. Lett. **105**, 036401 (2010).
[18] Y. Singh and D. C. Johnston, Phys. Rev. B **76**, 012407 (2007).
[19] A. A. Aczel, Y. Kohama, C. Marcenat, F. Weickert, M. Jaime, O. E. Ayala-Valenzuela, R. D. McDonald, S. D. Selesnic, H. A. Dabkowska, and G. M. Luke, Phys. Rev. Lett. **103**, 207203 (2009).

[20] M. Kofu, J.-H. Kim, S. Ji, S.-H. Lee, H. Ueda, Y. Qiu, H.-J. Kang, M. A. Green, and Y. Ueda, Phys. Rev. Lett. **102**, 037206 (2009).
[21] Z. Wang, M. Schmidt, A. Günther, S. Schaile, N. Pascher, F. Mayr, Y. Goncharov, D. L. Quintero-Castro, A. T. M. N. Islam, B. Lake, H.-A. Krug von Nidda, A. Loidl, and J. Deisenhofer, Phys. Rev. B **83**, 201102(R) (2011).
[22] L. N. Kantorovich, User-friendly visualization program for *ab initio* DFT codes VASP, SIESTA, QE, and QUICKSTEP, 1996–2012 (unpublished).
[23] M. Rabie, Ph.D. thesis, University of Madrid, 2012.
[24] H. Konno, H. Tachikawa, A. Furusaki, and R. Furuichi, Analyt. Sci. **8**, 641 (1992).
[25] K. Koepernik and H. Eschrig, Phys. Rev. B **59**, 1743 (1999).
[26] J. P. Perdew and Y. Wang, Phys. Rev. B **45**, 13244 (1992).
[27] J. Heyd, G. E. Scuseria, and M. Ernzerhof, J. Chem. Phys. **118**, 8207 (2003). J. Heyd and G. E. Scuseria, *ibid.* **121**, 1187 (2004).
[28] G. Kresse and J. Furthmüller, Comput. Mater. Sci. **6**, 15 (1996). Phys. Rev. B **54**, 11169 (1996).
[29] J. Uddin and G. E. Scuseria, Phys. Rev. B **74**, 245115 (2006).
[30] L. Li, W. Yu, and C. Jin, Phys. Rev. B **73**, 174115 (2006).
[31] P. Blaha, K. Schwarz, G. K. H. Madsen, D. Kvasnicka, and J. Luitz, WIEN2K, an augmented plane wave + local orbitals program for calculating crystal properties, Techn. Universität Wien, Getreidemarkt 9/156A, 1060 Wien, Austria, 2001.
[32] V. I. Anisimov, J. Zaanen, and O. K. Andersen, Phys. Rev. B **44**, 943 (1991).
[33] V. I. Anisimov, I. V. Solovyev, M. A. Korotin, M. T. Czyzyk, and G. A. Sawatzky, Phys. Rev. B **48**, 16929 (1993).
[34] L. Chioncel, H. Allmaier, E. Arrigoni, A. Yamasaki, M. Daghofer, M. I. Katsnelson, and A. I. Lichtenstein, Phys. Rev. B **75**, 140406(R) (2007).
[35] E. Pavarini, S. Biermann, A. Poteryaev, A. I. Lichtenstein, A. Georges, and O. K. Andersen, Phys. Rev. Lett. **92**, 176403 (2004).
[36] The hopping integral $V(e)$ between a Cr orbital of e symmetry and its O $2p$ ligands in a CrO_4 tetrahedral cluster is about 3.05–3.30 eV according to LDA [$(pd\pi) = 1.87$–2.02 eV], while the hopping integral $V(t_{2g})$ between a t_{2g} orbital and its oxygen ligands in a CrO_6 octahedral cluster is substantially smaller, about 2.20 eV for $LaCrO_3$ [$(pd\pi) = 1.10$ eV].
[37] A. Maignan, V. Caignaert, B. Raveau, D. Khomskii, and G. Sawatzky, Phys. Rev. Lett. **93**, 026401 (2004).
[38] C. F. Chang, Z. Hu, H. Wu, T. Burnus, N. Hollmann, M. Benomar, T. Lorenz, A. Tanaka, H.-J. Lin, H. H. Hsieh, C. T. Chen, and L. H. Tjeng, Phys. Rev. Lett. **102**, 116401 (2009).